

Table I. Combination index value of the interaction between CDDP with 17-AAG against human esophageal carcinoma cell lines.

Cell line	IC ₅₀ of 17-AAG (μM)	Concentration of 17-AAG (μM)	CI at IC ₅₀	Interpretation
KYSE30	2.37	1.000	0.49	Synergism
		0.500	0.76	Moderate synergism
KYSE150	0.10	0.050	0.71	Moderate synergism
		0.025	0.55	Synergism
EC-GI-10	1.40	1.000	1.80	Antagonism
		0.500	1.78	Antagonism
TE6	0.04	0.050	1.18	Moderate antagonism
		0.025	1.06	Additive effect

Different concentrations of 17-AAG were employed to study the effect on IC₅₀ of CDDP. Variable ratios of drug concentrations and mutually non-exclusive equations were used to determine the CI. CI > 1.3 indicates antagonism; CI = 1.1 to 1.3, moderate antagonism; CI = 0.9 to 1.1, additive effect; CI = 0.8 to 0.9, slight synergism; CI = 0.6 to 0.8, moderate synergism; CI = 0.4 to 0.6, synergism; and CI = 0.2 to 0.4, strong synergism. CI, combination index; CDDP, cisplatin.

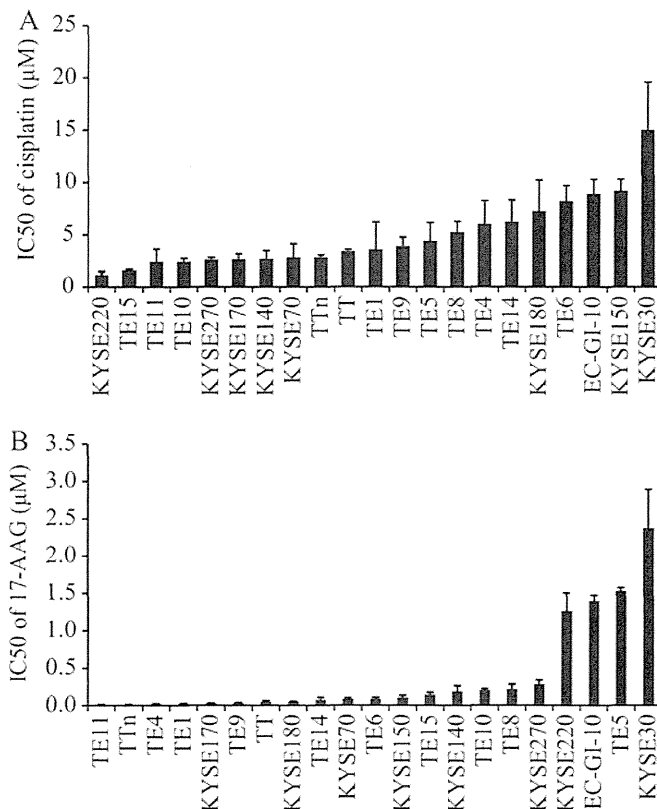


Figure 1. IC₅₀ values for cisplatin (A) and 17-AAG (B) across the panel of esophageal squamous cell carcinoma cell lines. Cells were treated with a range of concentrations of cisplatin or 17-AAG for 72 h. Viable cell density was determined by a water-soluble tetrazolium salt and IC₅₀ was calculated. The values and error bars represent the mean and standard deviation of at least three experiments performed in quintuplicate.

lines, KYSE30, KYSE150, EC-GI-10 and TE6 were treated with various concentrations of each drug alone or in combination, and were then subjected to a cell viability assay. As shown in Fig. 2, the combination with low-dose 17-AAG shifted the survival curve to the left in KYSE30 and KYSE150. The

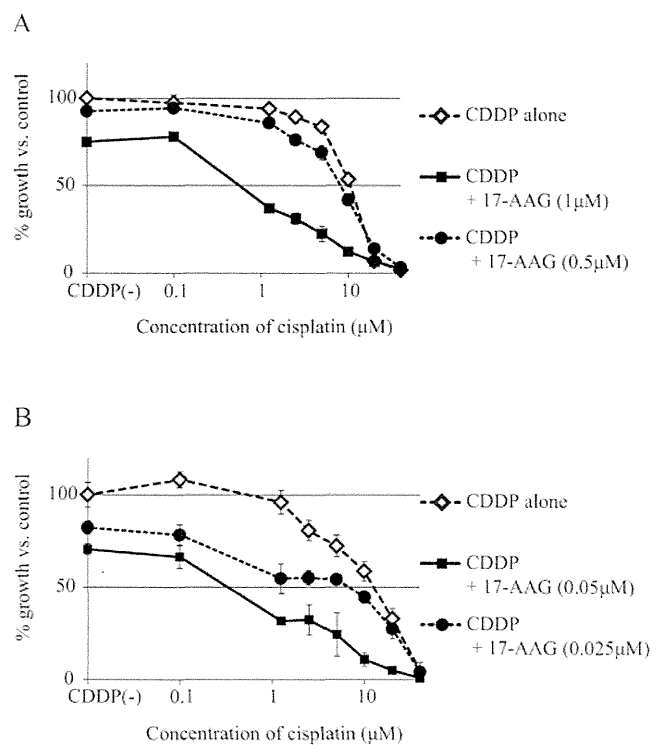


Figure 2. Dose-response curve for cisplatin (CDDP) in the presence of low doses of 17-AAG. KYSE30 and KYSE150 were treated with various doses of CDDP (0.1-40 μM) and 17-AAG (0.5-1 μM for KYSE30; 0.025-0.05 μM for KYSE150) for 72 h, and cytotoxicity was evaluated by a drug sensitivity assay. (A) KYSE30, (B) KYSE150. The experiment was performed twice and representative data are shown. Data are presented as means ± standard deviation of quintuplicate wells.

interaction between CDDP and 17-AAG was determined by calculating the CI. The CI values of KYSE30 and KYSE150 ranged from 0.4 to 0.7 for 50% cell kill, demonstrating synergistic behavior between CDDP and 17-AAG (Table I). In contrast, the CI value of EC-GI-10 and TE6 ranged from 1.0 to 1.8.

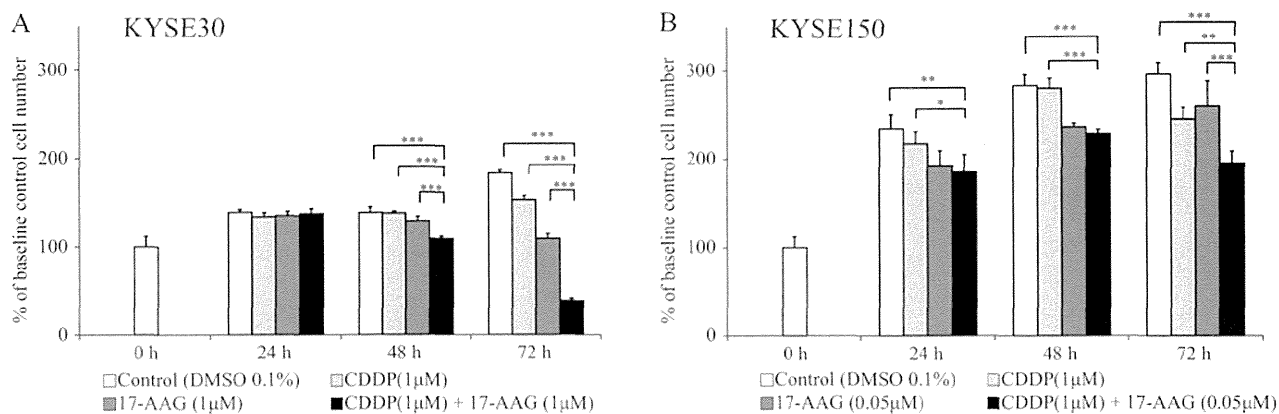


Figure 3. Changes in cell numbers by the treatment with cisplatin (CDDP) and 17-AAG, alone or in combination. (A) KYSE30 and (B) KYSE150 were exposed to 17-AAG alone (1 μ M for KYSE30, 0.05 μ M for KYSE150), CDDP alone (1 μ M for both cell lines), and the combination of CDDP (1 μ M for both cell lines) and 17-AAG (1 μ M for KYSE30, 0.05 μ M for KYSE150). Cell numbers were counted after 24, 48 and 72 h. Data are presented as means and standard deviation of quintuplicate wells. * P <0.05, ** P <0.01, *** P <0.001.

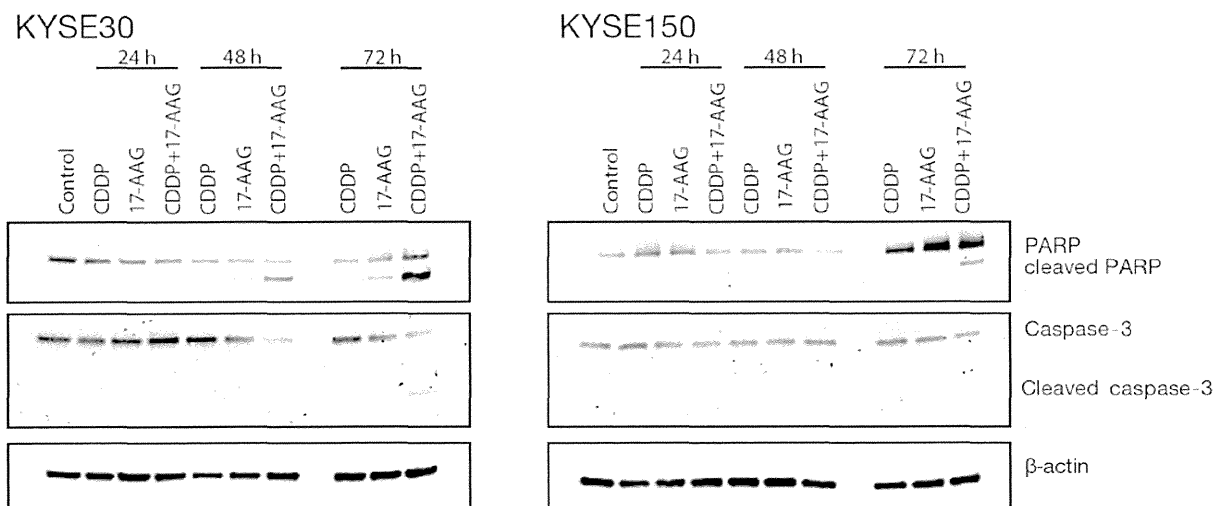


Figure 4. Induction of apoptosis by the combination of cisplatin (CDDP) and 17-AAG. KYSE30 was treated with CDDP (1 μ M) and/or 17-AAG (1 μ M), while KYSE150 was treated with CDDP (1 μ M) and/or 17-AAG (0.05 μ M). After the treatment, cell extracts were examined by western blot analysis.

These results showed either the additive or antagonistic effects of CDDP and 17-AAG in EC-GI-10 and TE6.

Cell count assay. To confirm the synergistic effect of CDDP and 17-AAG in KYSE30 and KYSE150, we counted actual cell numbers after treatment with the vehicle only (0.1% DMSO), 1 μ M CDDP only, 1 μ M 17-AAG only, and the combined treatment with 1 μ M CDDP and 1 μ M 17-AAG for 24, 48 and 72 h.

As shown in Fig. 3, low-dose CDDP alone and low-dose 17-AAG alone modestly suppressed cell growth in KYSE30 and KYSE150 (Fig. 3). However, the reduction in cell growth was significantly greater with the combination of CDDP and 17-AAG than with either drug alone.

Combination of CDDP and 17-AAG induces apoptosis. Using western blot analysis, we determined whether the reduced cell growth caused by the combined treatment with CDDP and 17-AAG occurred due to the induction of apoptosis via the cleavage of poly (ADP-ribose) polymerase (PARP) and activation of caspase-3.

No significant changes were observed in the expression of PARP and cleaved PARP 24 h after treatment with CDDP alone, 17-AAG alone, or CDDP and 17-AAG (Fig. 4). However, a clear increase was observed in cleaved PARP 48 h after the co-treatment with CDDP and 17-AAG in KYSE30 and KYSE150. The increase in cleaved PARP was greater than that with either drug alone. The induction of cleaved PARP was further enhanced at 72 h. Cleaved caspase-3 was detected 72 h after the co-treatment with CDDP and 17-AAG in KYSE30, but the band was weaker than that of cleaved PARP.

Combination of CDDP and 17-AAG reduces the expression of XIAP and phosphorylated Akt. To understand the mechanism underlying the synergy between CDDP and 17-AAG, we investigated the expression of proteins associated with apoptosis (Fig. 5). Under basal conditions, KYSE30 expressed high levels of XIAP, cIAP1, and survivin and low levels of cIAP2. KYSE150 expressed high levels of XIAP and cIAP1, and low levels of cIAP2 and survivin. Livin was not detected in either cell line.

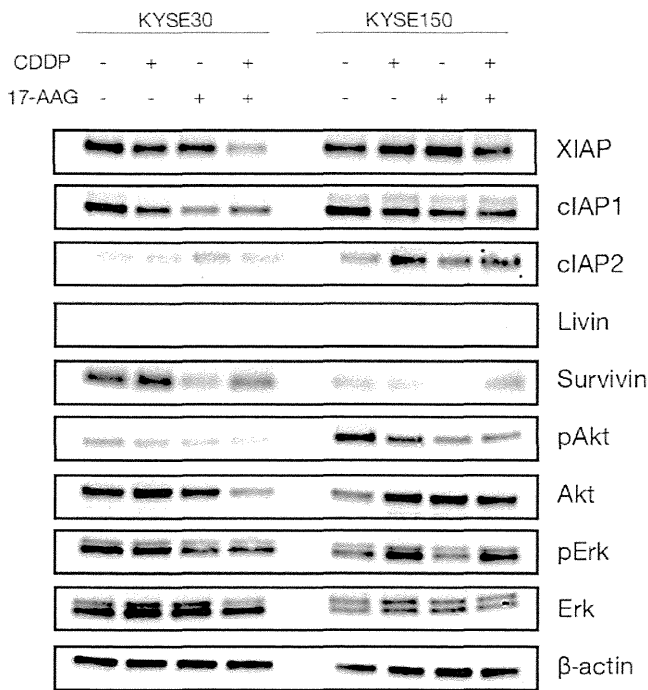


Figure 5. Western blot analysis of the IAP family proteins, the Erk and Akt pathways. KYSE30 and KYSE150 were treated with cisplatin (CDDP; 1 μ M), 17-AAG (1 μ M for KYSE30, 0.05 μ M for KYSE150), and the combination of these drugs for 72 h, and cell lysates were analyzed by western blotting.

The treatment with CDDP alone, 17-AAG alone, or combined treatment with CDDP and 17-AAG induced variable changes in the levels of cIAP1, cIAP2 and survivin; however, a correlation was not observed between these changes and cell growth inhibition or the induction of apoptosis by the treatment. XIAP levels were, in contrast, unchanged by either agent alone, but were significantly reduced by the combined treatment. We also examined the expression of Bcl-2 family members, including Bcl-2, Bcl-xL, Bid, Bad, Bax, Bim, Beclin and BAG-1; however, no significant changes were observed by the treatment with CDDP alone, 17-AAG alone, or combined treatment with CDDP and 17-AAG (data not shown). These

results demonstrated that the combination of CDDP and 17-AAG mainly induced apoptosis by inhibiting XIAP.

To identify the mechanism for the reduction in XIAP, the expression of the Akt and the Erk pathways was examined. As shown in Fig. 5, phosphorylated Akt levels were slightly reduced by either CDDP or 17-AAG alone in both cell lines. However, the combination of CDDP and 17-AAG clearly diminished phosphorylated Akt levels (Fig. 5). Phosphorylated Erk levels remained unchanged by the treatment in KYSE30. Phosphorylated Erk levels were modestly increased by CDDP alone and the combined treatment with CDDP and 17-AAG in KYSE150; however, no correlation was observed between these changes and the inhibition of cell growth or induction of apoptosis.

Time-dependent changes in the expression of phosphorylated Akt, total Akt, and XIAP. In order to determine time-dependent changes in phosphorylated Akt, total Akt and XIAP, we examined the expression of these proteins after the treatment with CDDP and/or 17-AAG, either alone or in combination (Fig. 6). Phosphorylated Akt levels were modestly reduced by 17-AAG alone and by the combination of CDDP and 17-AAG after 24 h. Further reductions occurred at 72 h, especially with the combination of CDDP and 17-AAG in KYSE30. The expression of phosphorylated Akt was not significantly changed by CDDP alone. The expression of XIAP was reduced by 17-AAG alone and by the combination of CDDP and 17-AAG, similar to that for phosphorylated Akt.

Discussion

In the present study, we demonstrated that the combined treatment with CDDP and 17-AAG had synergistic inhibitory effects on cell growth in CDDP-resistant ESCCs. The synergistic interaction between CDDP and 17-AAG resulted in significant increases in the cytotoxicity of CDDP; a strong cytotoxic effect was obtained in the presence of low-dose 17-AAG, which hardly has a cytotoxic effect by itself, in combination with a low concentration of CDDP. This cytotoxic effect occurred via induction of apoptosis, as demonstrated by the cleavage of PARP and caspase-3.

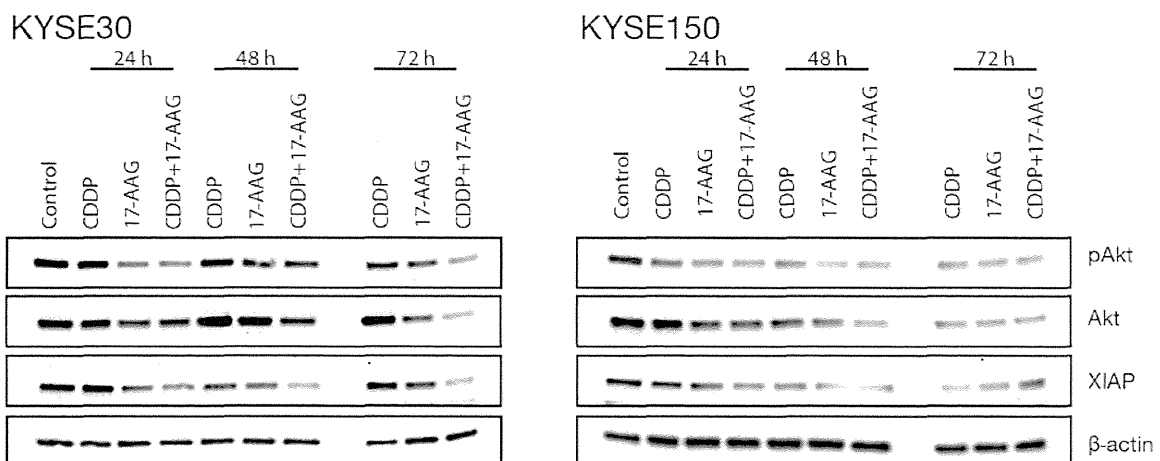


Figure 6. Time-dependent changes in the expression of phosphorylated Akt, Akt and XIAP. KYSE30 and KYSE150 were treated with cisplatin (CDDP; 1 μ M), 17-AAG (1 μ M for KYSE30, 0.05 μ M for KYSE150), and the combination of these drugs for the indicated times, and cell lysates were analyzed by western blotting.

The synergy between CDDP and an HSP90 inhibitor has been reported in previous studies; for example, McCollum *et al* reported that CDDP was synergistic with geldanamycin or 17-AAG and combined treatment with the two drugs increased apoptosis in the lung cancer cell line A549 (12). This synergy was attributed in part to the CDDP-induced abrogation of heat shock factor-1 activity. Weng *et al* also showed that 17-AAG enhanced CDDP cytotoxicity in the non-small cell lung cancer cell lines, A549 and H1650 (13). This synergistic effect was reported to be mediated by the downregulation of thymidine phosphorylase and Akt activation. We have yet to examine whether similar mechanisms occur in our cell lines. Nevertheless, our study provides the first evidence for the synergy of CDDP and 17-AAG in CDDP-resistant esophageal squamous cell lines.

We also revealed that, among the major regulators of apoptosis, the Akt/XIAP pathway mediated the synergistic effect of CDDP and 17-AAG; the expression patterns of phosphorylated Akt and XIAP levels closely correlated with their inhibitory effect on cell growth, induction of PARP cleavage, and apoptosis, which occurred by the combined treatment with CDDP and 17-AAG. Moreover, time-course experiments demonstrated that the reduction in phosphorylated Akt and XIAP levels were concomitant with the induction of PARP cleavage and apoptosis.

Previous studies indicated the Akt/XIAP pathway as the main regulator of apoptosis by chemotherapy in some cancer cell lines, including carcinomas of the breast, ovary, uterine cervix and melanoma (14-17). Akt phosphorylates and stabilizes XIAP, and the deactivation or knockdown of Akt destabilizes XIAP, leading to apoptosis (18). In addition, specific inhibition of XIAP expression was shown to induce apoptosis and increase caspase-3 activity in prostate cancer cells (19). These findings support our conclusion that the synergistic effect of CDDP and 17-AAG is mediated by the induction of apoptosis via the Akt and XIAP pathways.

One limitation of our study is that we lack data showing the synergy of CDDP and 17-AAG *in vivo*, and such data will be required to extrapolate the current results to clinical situations. We also cannot explain why synergy occurred in KYSE30 and KYSE150, but not in EC-GI-10 or TE6. A recent study indicated phosphatase and tensin homolog (PTEN) as a potential predictive marker for HSP90 inhibitor sensitivity among four ESCC cell lines (20). However, biomarkers that predict the HSP90 response or synergy of an HSP90 inhibitor and CDDP have not yet been established (21). The identification of such biomarkers is crucial in clinical settings.

In conclusion, we showed that the combination of low concentrations of CDDP with low-dose 17-AAG exerted synergistic effects on CDDP-resistant ESCC cell lines. The mechanism of the synergy was attributed to apoptosis mediated by downregulation of the Akt/XIAP pathway. Our results indicate that the co-administration of low-dose 17-AAG and CDDP overcomes CDDP chemoresistance and may improve the outcomes of patients with ESCC.

References

- Jemal A, Bray F, Center MM, Ferlay J, Ward E and Forman D: Global cancer statistics. *CA Cancer J Clin* 61: 69-90, 2011.
- Ozawa S, Tachimori Y, Baba H, *et al*: Comprehensive registry of esophageal cancer in Japan, 2004. *Esophagus* 9: 75-98, 2012.
- Miyata H, Yamasaki M, Kurokawa Y, *et al*: Multimodal treatment for resectable esophageal cancer. *Gen Thorac Cardiovasc Surg* 59: 461-466, 2011.
- Berrino F, De Angelis R, Sant M, *et al*: Survival for eight major cancers and all cancers combined for European adults diagnosed in 1995-99: results of the EURO CARE-4 study. *Lancet Oncol* 8: 773-783, 2007.
- Siegel R, Naishadham D and Jemal A: Cancer statistics, 2012. *CA Cancer J Clin* 62: 10-29, 2012.
- Yamasaki M, Miyata H, Tanaka K, *et al*: Multicenter phase I/II study of docetaxel, cisplatin and fluorouracil combination chemotherapy in patients with advanced or recurrent squamous cell carcinoma of the esophagus. *Oncology* 80: 307-313, 2011.
- Hara H, Tahara M, Daiko H, *et al*: Phase II feasibility study of preoperative chemotherapy with docetaxel, cisplatin, and fluorouracil for esophageal squamous cell carcinoma. *Cancer Sci*: Aug 30, 2013 (Epub ahead of print).
- Neckers L and Neckers K: Heat-shock protein 90 inhibitors as novel cancer chemotherapeutic agents. *Expert Opin Emerg Drugs* 7: 277-288, 2002.
- Newman B, Liu Y, Lee HF, Sun DX and Wang Y: HSP90 inhibitor 17-AAG selectively eradicates lymphoma stem cells. *Cancer Res* 72: 4551-4561, 2012.
- Zhang H and Burrows F: Targeting multiple signal transduction pathways through inhibition of Hsp90. *J Mol Med* 82: 488-499, 2004.
- Chou TC: Theoretical basis, experimental design, and computerized simulation of synergism and antagonism in drug combination studies. *Pharmacol Rev* 58: 621-681, 2006.
- McCollum AK, Lukasiewicz KB, Teneyck CJ, Lingle WL, Toft DO and Erlichman C: Cisplatin abrogates the geldanamycin-induced heat shock response. *Mol Cancer Ther* 7: 3256-3264, 2008.
- Weng SH, Tseng SC, Huang YC, Chen HJ and Lin YW: Inhibition of thymidine phosphorylase expression by using an HSP90 inhibitor potentiates the cytotoxic effect of cisplatin in non-small-cell lung cancer cells. *Biochem Pharmacol* 84: 126-136, 2012.
- Pramanik KC, Kudugunti SK, Fofaria NM, Moridani MY and Srivastava SK: Caffeic acid phenethyl ester suppresses melanoma tumor growth by inhibiting PI3K/AKT/XIAP pathway. *Carcinogenesis* 34: 2061-2070, 2013.
- Rajput S, Kumar BN, Sarkar S, *et al*: Targeted apoptotic effects of thymoquinone and tamoxifen on XIAP mediated Akt regulation in breast cancer. *PLoS One* 8: e61342, 2013.
- Gagnon V, Van Themsche C, Turner S, Leblanc V and Asselin E: Akt and XIAP regulate the sensitivity of human uterine cancer cells to cisplatin, doxorubicin and taxol. *Apoptosis* 13: 259-271, 2008.
- Asselin E, Mills GB and Tsang BK: XIAP regulates Akt activity and caspase-3-dependent cleavage during cisplatin-induced apoptosis in human ovarian epithelial cancer cells. *Cancer Res* 61: 1862-1868, 2001.
- Dan HC, Sun M, Kaneko S, *et al*: Akt phosphorylation and stabilization of X-linked inhibitor of apoptosis protein (XIAP). *J Biol Chem* 279: 5405-5412, 2004.
- Amantana A, London CA, Iversen PL and Devi GR: X-linked inhibitor of apoptosis protein inhibition induces apoptosis and enhances chemotherapy sensitivity in human prostate cancer cells. *Mol Cancer Ther* 3: 699-707, 2004.
- Bao XH, Takaoka M, Hao HF, *et al*: Antiproliferative effect of the HSP90 inhibitor NVP-AUY922 is determined by the expression of PTEN in esophageal cancer. *Oncol Rep* 29: 45-50, 2013.
- Garcia-Carbonero R, Carnero A and Paz-Ares L: Inhibition of HSP90 molecular chaperones: moving into the clinic. *Lancet Oncol* 14: e358-e369, 2013.



Original Article

Immunohistochemical analysis of the expression of E-cadherin and ZEB1 in non-small cell lung cancer

Daisuke Matsubara,^{1,2} Yuka Kishaba,² Taichiro Yoshimoto,² Yuji Sakuma,² Takashi Sakatani,² Tomoko Tamura,² Shunsuke Endo,⁴ Yukihiko Sugiyama,³ Yoshinori Murakami¹ and Toshiro Niki²

¹Molecular Pathology Laboratory, Institute of Medical Science, University of Tokyo, Tokyo, ²Department of Integrative Pathology, Divisions of ³Pulmonary Medicine and ⁴General Thoracic Surgery, Jichi Medical University, Tochigi, Japan

We performed an immunohistochemical analysis of the expression of zinc-finger E-box binding homeobox 1 (ZEB1), a master regulator of epithelial-mesenchymal transition (EMT), and determined its relationship with E-cadherin in 157 non-small cell lung carcinomas (93 adenocarcinomas, 36 squamous cell carcinomas, 18 large cell carcinomas, and 10 pleomorphic carcinomas). Although the expression of E-cadherin was low in the subset of adenocarcinomas (10%) and squamous cell carcinomas (11%), ZEB1 expression was only observed in one case of squamous cell carcinoma and none of the adenocarcinomas. In contrast, the low expression of E-cadherin (50% and 90%, respectively) and the positive expression of ZEB1 (11% and 50%, respectively) were more frequently observed in poorly differentiated carcinomas (large cell carcinomas and pleomorphic carcinomas). Overall, the expression of ZEB1 was inversely correlated with that of E-cadherin. Furthermore, the distribution of ZEB1-positive cancer cells was more restricted than in the area in which the expression of E-cadherin was lost, and the former was detected within the latter. We concluded that the expression of ZEB1 was not necessarily associated with the low expression of E-cadherin in lung adenocarcinomas and squamous cell carcinomas. The expression of ZEB1 correlated with an undifferentiated and/or sarcomatoid morphology that may occur in the late stage of EMT.

Key words: E-cadherin, EMT, lung adenocarcinoma, ZEB1

Lung cancer is the leading cause of cancer death in many developed countries, including the United States and Japan.^{1,2} Patients with lung carcinoma have a poor prognosis;

disease recurrence is frequently reported in most patients following complete surgical resection and the 5-year survival rate of those with stage I disease is only 70%.³

Epithelial-mesenchymal transition (EMT) is a phenomenon in which epithelial cells lose the epithelial phenotype and temporarily or permanently gain the mesenchymal phenotype, which has been correlated with embryonic development, wound healing, tissue regeneration, organ fibrosis, and carcinogenesis. The relationship between EMT and cancer invasion or metastasis has been demonstrated both *in vitro* and *in vivo*.⁴ Moreover, EMT in cancer has been associated with the stem cell phenotype,⁵ and also the acquisition of drug resistance.⁶ Recent evidence has suggested that EMT is regulated by master EMT-inducing transcriptional factors, including Snail, Twist, Zeb, and E47 (a), and, of these, zinc-finger E-box binding homeobox 1 (ZEB1) has been proposed as a major factor in the EMT process in lung cancer.^{7–9} ZEB1 appears to contribute to maintaining the aggressive phenotype of lung cancer, thereby promoting anchorage-independent proliferation,¹⁰ inhibiting tumor suppressor genes such as semaphorin 3F (SEMA3F),¹¹ and repressing EMT-inhibiting miR200 families.¹² However, most of the supportive findings on ZEB1 have been obtained using cell lines. Few studies have examined the expression of ZEB1 and its relationship to EMT in primary lung cancer tissues.

Therefore, we herein performed an immunohistochemical analysis of ZEB1 and E-cadherin using whole sections from 157 cases of non-small cell lung carcinoma, and attempted to elucidate the relationship between the expression of ZEB1 and E-cadherin and the pathomorphological features of EMT.

MATERIALS AND METHODS

Patients and tumors

Tumor specimens were obtained from 157 patients who underwent lung cancer surgery at the Jichi Medical University

Correspondence: Toshiro Niki, MD, PhD, Division of Integrative Pathology, Jichi Medical University, 3311-1, Yakushiji, Shimotsukeshi, Tochigi 329-0498, Japan. Email: tniki@jichi.ac.jp

Disclosure: There is no conflict of interest in this study.

Received 10 June 2014. Accepted for publication 9 September 2014.

© 2014 Japanese Society of Pathology and Wiley Publishing Asia Pty Ltd

hospital for adenocarcinomas ($n = 93$) and squamous cell carcinomas ($n = 36$) between 2005 and 2008, and for large cell carcinomas ($n = 18$) and pleomorphic carcinomas ($n = 10$) between 2005 and 2011. Informed consent was obtained from all patients, and the study was approved by the Institutional Ethics Review Committee. Patients included 105 males and 52 females, ranging in age from 38 to 86 years (average 66 years). Each case was reassigned according to the tumor, node, metastasis (TNM) classification and pathological stage on the basis of the new IASLC staging system.¹³ Ninety-two cases were classified as Stage I (69 Stage IA, 23 Stage IB), 31 were Stage II (10 Stage IIA, 21 Stage IIB), and 26 were Stage III (22 Stage IIIA, 4 Stage IIIB). Eight cases were identified as stage IV.

The tumors were cut at approximately 5-mm intervals after fixation in 10% formalin and embedded in paraffin. Adenocarcinomas were histologically subtyped according to the international multidisciplinary classification of lung adenocarcinoma by the International Association for the Study of Lung Cancer, American Thoracic Society, and European Respiratory Society.¹⁴ The histological criteria for vascular, lymphatic, and pleural invasion were as described previously.¹⁵

Immunohistochemistry

Specimens for the immunohistochemical evaluation were taken from representative areas of the tumor, including the largest cut surface. Sections of 5 μm thickness were cut and deparaffinized through graded xylene and ethanol. The sections were first treated with 0.3% hydrogen peroxide in methanol for 30 min to block endogenous peroxidase activity, and then autoclaved in 10 mM citrate buffer (pH 6.0) for 10 min at 120°C (for E-cadherin, and ZEB1). Sections were preincubated with 10% normal horse serum in phosphate-buffered saline, incubated with a mouse monoclonal antibody against E-cadherin (clone 36, BD Biosciences, Franklin Lakes, NJ, USA) at a dilution of 1:400, and a rabbit polyclonal antibody against ZEB1 (HPA027524, Sigma-Aldrich, St. Louis, MO, USA) at a dilution of 1:800 at 4°C overnight. The linked primary antibody was detected with the DAKO LSAB2 streptavidin-peroxidase system (Agilent technologies, Santa Clara, CA, USA) according to the manufacturer's instructions. 3,3'-diaminobenzidine tetrahydrochloride (DAB) was used as a chromogen, whereas hematoxylin was used as a light counterstain. No significant staining was observed in the negative controls, which were prepared using the same class of mouse immunoglobulin at the same concentration.

Evaluation of Immunohistochemistry

Immunohistochemical staining was evaluated by three pathologists (D.M, T.Y and T.N), independently, through light

microscopic observations and without knowledge of the clinical data of each patient. The concordance of the scores of ZEB1 and E-cadherin were 91% (143 of 157) and 81% (128 of 157), respectively. Cases of disagreement were reviewed jointly to reach a consensus score.

ZEB1 and E-cadherin immunoreactivities were evaluated as follows. Nuclear staining was assessed for ZEB1, while membranous and cytoplasmic staining was assessed for E-cadherin. Immunoreactivity was evaluated semiquantitatively based on the intensity and estimated percentage of tumor cells that were stained. Intensity was quantified as follows: 1+ , weak staining (detection required high magnification); 2+ , moderate staining (detected readily at medium magnification); 3+ , strong staining (detected readily at low magnification). The percentages of positive cells were scored into five categories: 0, 0%; 1, 1–25%; 2, 26–50%; 3, 51–75%; and 4, 76–100%. The product of the intensity and percentage scores was used as the final staining score. The final score for the staining of ZEB1 was defined as negative expression (final staining score <2) and positive expression (final staining score \geq 2). Positive staining of ZEB1 was observed in the stromal fibroblasts used as internal control. The final score for the staining of E-cadherin was defined as low-level expression (final staining score <8) and high-level expression (final staining score \geq 8).

Statistics

The chi-squared test and multivariate logistic regression analysis were used to evaluate clinicopathological correlations. Results were considered significant if the *P* value was less than 0.05. All statistical calculations were performed using the StatView computer program (Abacus Concepts, Berkeley, CA, USA).

RESULTS

E-cadherin and ZEB1 expression patterns in lung adenocarcinomas

All tumor cells in most lung adenocarcinomas stained positive for E-cadherin, whereas the partial loss of E-cadherin staining was frequently observed in high-grade subtypes such as solid predominant adenocarcinomas and invasive mucinous adenocarcinomas, as shown in Fig. 1. Tables 1 and S1 show correlations between the expression of E-cadherin and Zeb1 in lung adenocarcinomas as a whole and each subtype of lung adenocarcinomas. Of the 93 lung adenocarcinoma cases, the expression of E-cadherin was high in 84 cases (90%) and low in 9 cases (10%). The 9 cases with low expression levels of E-cadherin consisted of 7 of 13 solid predominant adenocarcinomas (54%), 1 of 3 invasive

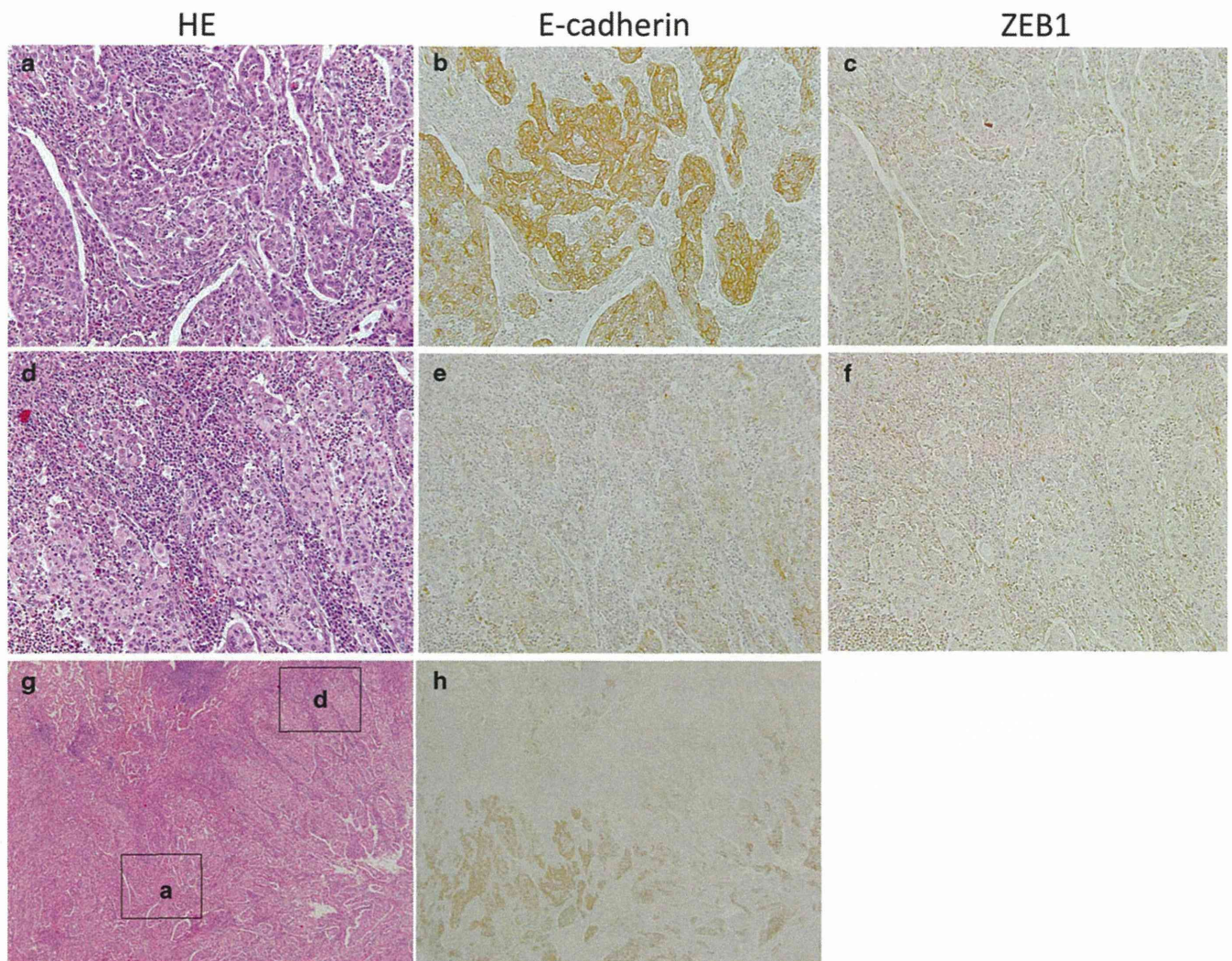


Figure 1 Staining of serial sections obtained from a case of poorly differentiated adenocarcinoma with solid components for HE, E-cadherin, and zinc-finger E-box binding homeobox 1 (ZEB1). (a–c) are higher magnifications of the staining for HE, E-cadherin, and ZEB1 in the E-cadherin positive area, respectively (magnification $\times 200$). (d–f) are higher magnifications of the staining for HE, E-cadherin, and ZEB1 in the area in which the expression of E-cadherin was lost, respectively (magnification $\times 200$). (g,h) show the staining for HE and E-cadherin in a low power field, respectively (magnification $\times 20$). Although the tumor showed an overall poorly differentiated morphology, a more solid growth pattern was observed in the E-cadherin negative area (c) than in the E-cadherin positive part (a,b). ZEB1 was positive in stromal cells, but was negative in lung adenocarcinoma components (c,f), even in areas in which the expression of E-cadherin was low (f).

mucinous adenocarcinomas (33%), and 1 of 35 papillary predominant adenocarcinomas (3%). Some cases with high expression levels of E-cadherin showed not a predominant but a small foci of solid adenocarcinoma component, which frequently showed lower intensity of E-cadherin compared with other predominant components such as adenocarcinoma in situ, papillary, or acinar components in the same tumors. The cancer cells in all 93 lung adenocarcinoma cases, including the 9 cases with the low expression levels of E-cadherin, were negative for ZEB1 (Fig. 1c,f).

We compared the expression levels of E-cadherin with clinicopathological factors in lung adenocarcinomas (Table 2). Low expression levels of E-cadherin were corre-

lated with pleural invasion ($P = 0.0089$) and heavy smoking ($P = 0.0321$). Patients with low expression levels of E-cadherin had a slightly advanced T-factor ($P = 0.0700$).

E-cadherin and ZEB1 expression patterns in squamous cell carcinomas

The expression patterns of E-cadherin and ZEB1 in squamous cell carcinomas ($n = 36$) are shown in Table 1. Of the 36 squamous cell carcinoma cases, the expression of E-cadherin was high while that of ZEB1 was negative in 32 cases (89%). The expressions of E-cadherin and ZEB1 were

low and negative, respectively, in three cases (8%). The expression of E-cadherin was low while that of ZEB1 was positive in one case (3%), in which spindle cell cancer cell components accounted for less than 10% of all the tumor

Table 1 Expression levels of E-cadherin and zinc-finger E-box binding homeobox 1 (ZEB1) in histological subtypes of non-small cell carcinomas

Subtypes	E-cadherin high	E-cadherin low
Adenocarcinoma		
ZEB1 positive	0	0
ZEB1 negative	84	9
Squamous cell carcinoma		
ZEB1 positive	0	1
ZEB1 negative	32	3
Large cell carcinoma		
ZEB1 positive	0	2
ZEB1 negative	9	7
Pleomorphic carcinoma		
ZEB1 positive	0	5
ZEB1 negative	1	4

cells (Fig. 2). In this ZEB1 positive case, ZEB1 was negative and E-cadherin was positive in well to moderately differentiated squamous cell carcinoma components (Fig. 2a–c), while ZEB1 was positive and E-cadherin was negative in poorly differentiated squamous cell carcinoma components with spindle cell differentiation (Fig. 2d–f).

We compared the expression levels of E-cadherin and ZEB1 with clinicopathological factors in squamous cell carcinomas, but found no correlations (Table 3).

E-cadherin and ZEB1 expression patterns in large cell carcinomas and pleomorphic carcinomas

Of the 18 large cell carcinoma cases, the expression of E-cadherin was high while that of ZEB1 was negative in nine cases (50%), and the expression of E-cadherin was low while that of ZEB1 was positive in two cases (11%), which consisted of one case showing strong positivity of ZEB1 (score = 6) with about 70% positive cells and another case showing

Table 2 Correlations between expression levels of E-cadherin and zinc-finger E-box binding homeobox 1 (ZEB1) and clinico-pathological factors in adenocarcinomas

	E-cadherin expression			ZEB1 expression		
	high	low	<i>P</i> -value	positive	negative	<i>P</i> -value
Pathological stage						
I	62	5	0.2462	0	67	n.s.
II+III+IV	22	4		0	26	
T-stage						
T1	54	3	0.0700	0	57	n.s.
T2,T3,T4	30	6		0	36	
Nodal involvement (†)						
Positive	19	2	0.9070	0	21	n.s.
Negative	63	6		0	69	
Lymphatic invasion						
Positive	21	2	0.8544	0	23	n.s.
Negative	63	7		0	70	
Vessel invasion						
Positive	24	4	0.3239	0	28	n.s.
Negative	60	5		0	65	
Pleural invasion						
Positive	21	6	0.0089	0	27	n.s.
Negative	63	3		0	66	
Dissemination						
Positive	4	1	0.4222	0	5	n.s.
Negative	80	8		0	88	
Pulmonary metastasis						
Positive	3	1	0.2893	0	4	n.s.
Negative	81	8		0	89	
Tumor size						
3 cm ≤	21	3	0.5871	0	24	n.s.
3 cm >	63	6		0	69	
Smoking index						
600 ≤	26	6	0.0321	0	32	n.s.
600 >	58	3		0	61	

Bold values indicate those that are statistically significant.

n.s., not specified.

†Pathological N-factors were not determined for three cases of stage IV patients with pleural dissemination.

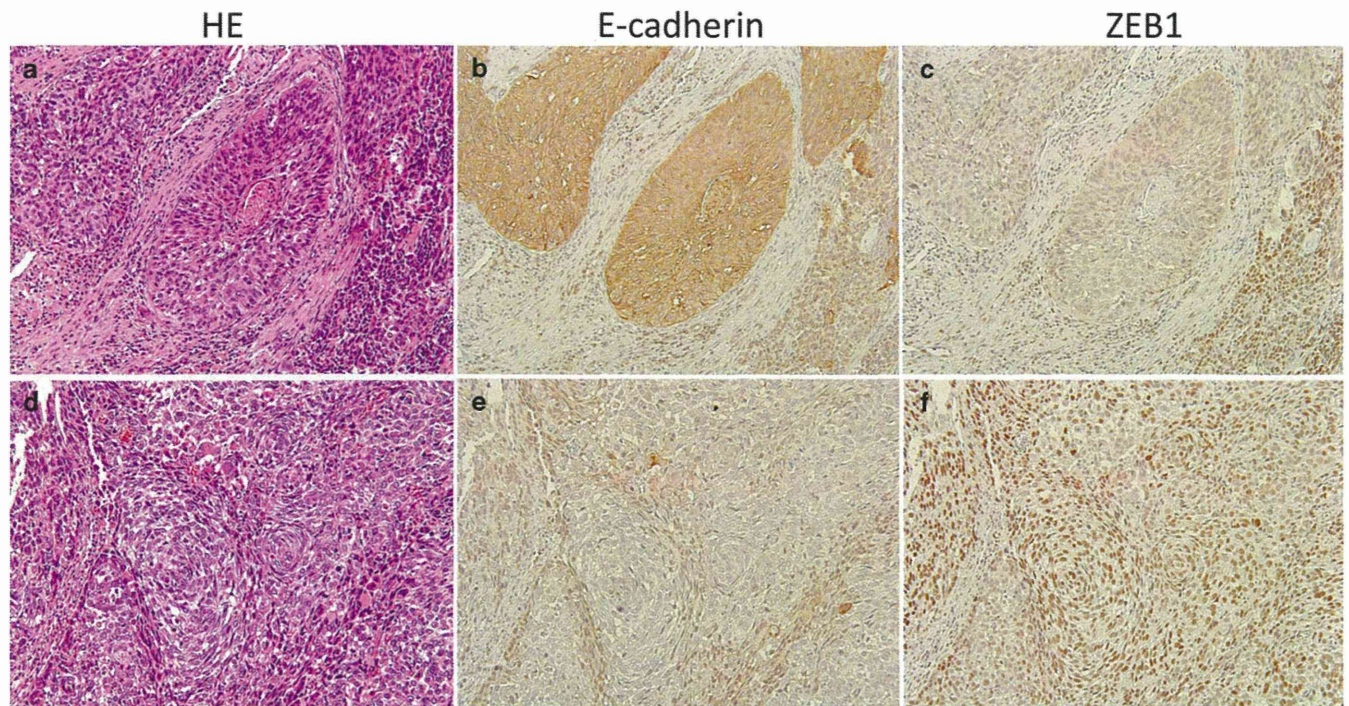


Figure 2 Staining of serial sections from a case of squamous cell carcinoma with spindle cell components less than 10% for HE, E-cadherin, and zinc-finger E-box binding homeobox 1 (ZEB1). (a–c) are higher magnifications of the staining for HE, E-cadherin, and ZEB1 in the E-cadherin positive part, respectively (magnification $\times 200$). (d–f) are higher magnifications of the staining for HE, E-cadherin, and ZEB1 in the part in which the expression of E-cadherin was lost, respectively (magnification $\times 200$). ZEB1 was negative and E-cadherin was positive in well to moderately differentiated squamous cell carcinoma components, while ZEB1 was positive and E-cadherin was negative in poorly differentiated squamous cell carcinoma components with spindle cell differentiation.

weak positivity (score = 2) of ZEB1 with less than 10% positive cells. The expressions of ZEB1 and E-cadherin were negative and low, respectively, in seven cases (39%) (Table 1). No case had high expression level of E-cadherin and positive expression of ZEB1, simultaneously.

Of the ten pleomorphic carcinoma cases, the expression of E-cadherin was high while that of ZEB1 was negative in one case (10%), and the expression of E-cadherin was low while that of ZEB1 was positive in five cases (50%), which consisted of four cases showing strong positivity of ZEB1 (score ≥ 6) with more than 50% positive cells and one case showing weak positivity (score = 2) of ZEB1 with less than 10% positive cells. The expressions of ZEB1 and E-cadherin were negative and low, respectively, in four cases (40%). No case had high expression level of E-cadherin and positive expression of ZEB1, simultaneously.

In individual cases of large cell carcinomas and pleomorphic carcinomas, ZEB1-positive portions were included in areas in which the expression of E-cadherin was low or negative, and we could not detect any part in which the expression of both ZEB1 and E-cadherin was simultaneously positive (Fig. 3). ZEB1-positive portions were negative for E-cadherin (Fig. 3g–i), while we detected parts in which the expression of E-cadherin was low in an area that was negative for ZEB1 (Fig. 3d–f).

We compared the expression levels of E-cadherin and ZEB1 with clinicopathological factors in large cell carcinomas and pleomorphic carcinomas (Table 4). The low expression of E-cadherin was correlated with larger tumors ($P = 0.0456$). Cases in which the expression of E-cadherin was low has a slightly more advanced pathological stage and advanced T-factor ($P = 0.0944$, $P = 0.0742$, respectively). Cases in which the expression of ZEB1 was positive were correlated with a lower frequency of vessel invasion ($P = 0.0078$) (Table 4).

Overall analysis of non-small cell carcinoma

The expression of ZEB1 was not necessarily related to the clinicopathological parameters associated with malignant potential or progression in the individual histological subtypes. However, when all non-small cell carcinoma cases were combined and analyzed as a whole, the expression of ZEB1 was inversely correlated with that of E-cadherin ($P < 0.0001$, chi-squared test), and the positive expression of ZEB1, as well as the lower expression of E-cadherin were positively correlated with an advanced pathological T-factor and stage, pleural invasion, larger tumors, and heavy smoking (Table S2). The expression of ZEB1 was more fre-

Table 3 Correlations between expression levels of E-cadherin and ZEB1 and clinico-pathological factors in pulmonary squamous cell carcinoma

	E-cadherin expression			ZEB1 expression		
	High	Low	<i>P</i> -value	Positive	Negative	<i>P</i> -value
Pathological stage						
I	12	2	0.6287	1	13	0.2036
II+III+IV	20	2		0	22	
T-stage						
T1	9	2	0.3706	0	11	0.5011
T2,T3,T4	23	2		1	24	
Nodal involvement						
Positive	12	1	0.6236	0	13	0.4458
Negative	20	3		1	22	
Lymphatic invasion						
Positive	10	1	0.7981	0	11	0.5011
Negative	22	3		1	24	
Vessel invasion						
Positive	18	1	0.2379	0	19	0.2836
Negative	14	3		1	16	
Pleural invasion						
Positive	11	1	0.7077	0	12	0.4733
Negative	21	3		1	23	
Dissemination						
Positive	0	0	n.s.	0	0	n.s.
Negative	32	4		1	35	
Pulmonary metastasis						
Positive	2	0	0.6069	0	2	0.8057
Negative	30	4		1	33	
Tumor size						
3 cm≤	21	3	0.7077	1	23	0.4733
3 cm>	11	1		0	12	
Smoking Index						
600≤	28	3	0.4955	1	30	0.6838
600>	4	1		0	5	

n.s., not specified.

quently observed in large cell carcinomas (LC) and pleomorphic carcinomas (PC) than in adenocarcinomas (AD) and squamous cell carcinomas (SQ) ($P < 0.0001$, shown in Table S2). In the multivariate analysis, however, only histology (LC + PC vs AD + SQ) remained significant, among the clinicopathological factors statistically correlated with the positive expression of ZEB1 (Table S3).

These results suggested that ZEB1 may be closely related to further dedifferentiation and sarcomatoid morphology.

DISCUSSION

In the present study, we performed an immunohistochemical analysis of E-cadherin and ZEB1 using 157 non-small cell lung carcinoma cases, including adenocarcinoma, squamous cell carcinoma, large cell carcinoma, and pleomorphic carcinoma. ZEB1 is one of the master transcriptional factors of EMT, and numerous studies have reported the key role of ZEB1 in the suppression of E-cadherin and induction of EMT.^{9,10,16} Therefore, we expected a close correlation between the expression

of ZEB1 and loss of E-cadherin. However, the expression of ZEB1 was not necessarily detected in cases with low expression levels of E-cadherin. The partial loss of E-cadherin was frequently observed in high-grade adenocarcinoma cases, such as invasive solid adenocarcinoma and invasive mucinous adenocarcinoma, whereas all adenocarcinoma cases including the high-grade subtypes were completely negative for ZEB1. The expression of ZEB1 was only observed in pleomorphic carcinoma, large cell carcinoma, or squamous cell carcinoma with spindle cell carcinoma components less than 10%. Moreover, ZEB1-positive cancer cells were restricted in their distribution and localized within the area of E-cadherin-low/negative cancer cells. These results suggested that ZEB1 may not be necessary to suppress the expression of E-cadherin in the early stage of EMT, but may be required to reinforce and perpetuate EMT in the late stage of tumor progression, in which tumor cells continue to lose epithelial traits and exhibit a sarcomatoid morphology. This hypothesis is consistent with the finding that the loss of E-cadherin resulted in the induction of multiple transcription factors, including TWIST and ZEB1.¹⁷

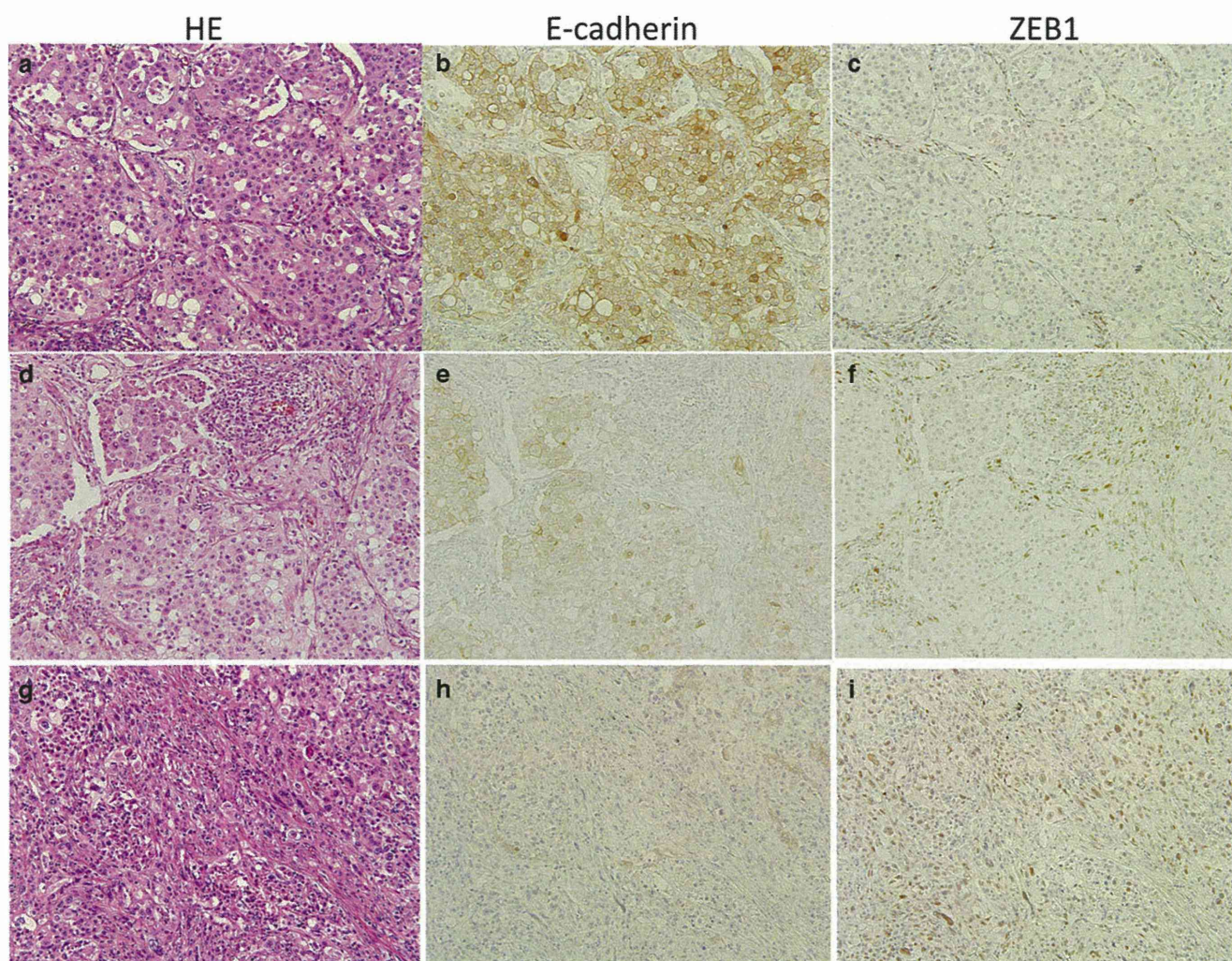


Figure 3 Staining of serial sections from a case of pleomorphic carcinoma for HE, E-cadherin, and zinc-finger E-box binding homeobox 1 (ZEB1). (a,d,g) show HE staining, (b,e,h) show the expression of E-cadherin, and (c,f,i) show the expression of ZEB1, in a high power field (magnification $\times 200$). ZEB1 was positive in the stromal cells surrounding cancer cell nests (c,f,i). The area with the high expression level of E-cadherin was negative for ZEB1 (a–c). Some areas with low expression levels of E-cadherin were negative for ZEB1 (d–f). The ZEB1-positive portion was completely negative for E-cadherin, and frequently showed a sarcomatoid morphology (g–i).

Pleomorphic carcinomas that exhibit a spindle cell or giant cell morphology may represent primary lung carcinomas that have acquired a ‘mesenchymal’ morphology. However, the concept of EMT is more widely used in the literature,¹⁸ and may encompass different phenomena or categories, such as: (i) tumor budding at the invasive front; (ii) de-differentiation; (iii) sarcomatoid changes; and (iv) specific types of cancer such as breast lobular carcinoma or gastric scirrhous carcinoma. For example, tumor budding at the invasive front of colorectal cancer is often referred to as EMT.¹⁹ Furthermore, the loss of E-cadherin is frequently reported in invasive solid adenocarcinoma, a high histological grade subtype, which can be presumed to result from EMT.²⁰ In all events, the loss of E-cadherin is a common feature of EMT; however, it is possible that EMT is not a single entity, but rather a hetero-

geneous phenomenon. EMT can be either reversible or irreversible and may occur via multiple steps and/or pathways. The degree of the loss of the epithelial phenotype may differ in different types of EMT, and the underlying molecular mechanisms may not be the same. For example, EMT-inducing transcription factors other than ZEB1, such as SNAIL, SLUG, and TWIST, may play a role in the different types of EMT in lung cancer. However, our experience with commercially available antibodies to these molecules, especially SNAIL, indicates that these antibodies may not be entirely specific, and we could not include data regarding expression of SNAIL, SLUG, etc, in the current study. We intend to address these issues in future studies by investigating the expression patterns of these EMT-inducing transcription factors in a more comprehensive manner.

Table 4 Correlations between expression levels of E-cadherin and ZEB1 and clinico-pathological factors in poorly differentiated carcinomas including large cell carcinomas and pleomorphic carcinomas

	E-cadherin expression			ZEB1 expression		
	High	Low	<i>P</i> -value	Positive	Negative	<i>P</i> -value
Pathological stage						
I	6	5	0.0944	1	10	0.1179
II+III+IV	4	13		6	11	
T-stage						
T1	4	2	0.0742	0	6	0.1106
T2,T3,T4	6	16		7	15	
Nodal involvement						
Positive	2	3	0.8792	1	4	0.8947
Negative	8	14		5	17	
Lymphatic invasion						
Positive	3	2	0.2111	0	5	0.1543
Negative	7	16		7	16	
Vessel invasion						
Positive	9	13	0.2720	3	19	0.0078
Negative	1	5		4	2	
Pleural invasion						
Positive	5	14	0.1315	6	13	0.2428
Negative	5	4		1	8	
Dissemination						
Positive	0	2	0.2740	1	1	0.3968
Negative	10	16		6	20	
Pulmonary metastasis						
Positive	0	2	0.2740	0	2	0.3968
Negative	10	16		7	19	
Tumor size						
3 cm≤	4	14	0.0456	6	12	0.1719
3 cm>	6	4		1	9	
Smoking Index						
600≤	9	17	0.1840	7	19	0.5466
600>	1	0		0	1	

Bold values indicate those that are statistically significant.
n.s., not specified

ACKNOWLEDGMENTS

This study was supported in part by JSPS KAKENHI Grant Number 20390103, JSPS KAKENHI Grant Number 25460432, Grants for Research on Human Genome Tailor-made from the Ministry of Health, Labor, and Welfare of Japan, and the Smoking Research Foundation.

REFERENCES

- 1 Statistics and Information Department. *Vital Statistics, 2000*. Tokyo: Ministry of Health, Labor and Welfare, 2001.
- 2 Jemal A, Siegel R, Ward E *et al*. Cancer statistics, 2006. *CA Cancer J Clin* 2006; **56**: 106–30.
- 3 Naruke T, Tsuchiya R, Kondo H *et al*. Prognosis and survival after resection for bronchogenic carcinoma based on the 1997 TNM-staging classification: The Japanese experience. *Ann Thorac Surg* 2001; **71**: 1759–64.
- 4 Yilmaz M, Christofori G. EMT, the cytoskeleton, and cancer cell invasion. *Cancer Metastasis Rev* 2009; **28**: 15–33.
- 5 Mani SA, Guo W, Liao MJ *et al*. The epithelial-mesenchymal transition generates cells with properties of stem cells. *Cell* 2008; **133**: 704–15.
- 6 Sequist LV, Waltman BA, Dias-Santagata D *et al*. Genotypic and histological evolution of lung cancers acquiring resistance to EGFR inhibitors. *Sci Transl Med* 2011; **3**: 75ra26.
- 7 Yang J, Mani SA, Donaher JL *et al*. Twist, a master regulator of morphogenesis, plays an essential role in tumor metastasis. *Cell* 2004; **117**: 927–39.
- 8 Moreno-Bueno G, Cubillo E, Sarrió D *et al*. Genetic profiling of epithelial cells expressing E-cadherin repressors reveals a distinct role for Snail, Slug, and E47 factors in epithelial-mesenchymal transition. *Cancer Res* 2006; **66**: 9543–56.
- 9 Ohira T, Gemmill RM, Ferguson K *et al*. WNT7a induces E-cadherin in lung cancer cells. *Proc Natl Acad Sci U S A* 2003; **100**: 10429–34.
- 10 Takeyama Y, Sato M, Horio M *et al*. Knockdown of ZEB1, a master epithelial-to-mesenchymal transition (EMT) gene, suppresses anchorage-independent cell growth of lung cancer cells. *Cancer Lett* 2010; **296**: 216–24.
- 11 Clarhaut J, Gemmill RM, Potiron VA *et al*. ZEB-1, a repressor of the semaphorin 3F tumor suppressor gene in lung cancer cells. *Neoplasia* 2009; **11**: 157–66.
- 12 Ceppi P, Mudduluru G, Kumarswamy R *et al*. Loss of miR-200c expression induces an aggressive, invasive, and chemoresistant phenotype in non-small cell lung cancer. *Mol Cancer Res* 2010; **8**: 1207–16.
- 13 Goldstraw P, Crowley J, Chansky K *et al*. The IASLC Lung Cancer Staging Project: Proposals for the revision of the TNM

- stage groupings in the forthcoming (seventh) edition of the TNM Classification of malignant tumours. *J Thorac Oncol* 2007; **2**: 706–14.
- 14 Travis WD, Brambilla E, Noguchi M *et al.* International Association for the Study of Lung Cancer/American Thoracic Society/European Respiratory Society international multidisciplinary classification of lung adenocarcinoma. *J Thorac Oncol* 2011; **6**: 244–85.
- 15 Matsubara D, Morikawa T, Goto A *et al.* Subepithelial myofibroblast in lung adenocarcinoma: A histological indicator of excellent prognosis. *Mod Pathol* 2009; **22**: 776–85.
- 16 Gemmill RM, Roche J, Potiron VA *et al.* ZEB1-responsive genes in non-small cell lung cancer. *Cancer Lett* 2011; **300**: 66–78.
- 17 Onder TT, Gupta PB, Mani SA *et al.* Loss of E-cadherin promotes metastasis via multiple downstream transcriptional pathways. *Cancer Res* 2008; **68**: 3645–54.
- 18 De Craene B, Berx G. Regulatory networks defining EMT during cancer initiation and progression. *Nat Rev Cancer* 2013; **13**: 97–110.
- 19 Oshiro R, Yamamoto H, Takahashi H *et al.* C4.4A is associated with tumor budding and epithelial-mesenchymal transition of colorectal cancer. *Cancer Sci* 2012; **103**: 1155–64.
- 20 Matsubara D, Kishaba Y, Ishikawa S *et al.* Lung cancer with loss of BRG1/BRM, shows epithelial mesenchymal transition phenotype and distinct histologic and genetic features. *Cancer Sci* 2013; **104**: 266–73.

SUPPORTING INFORMATION

Additional Supporting Information may be found in the online version of this article at the publisher's web-site:

Table S1 Expression levels of E-cadherin and ZEB1 in the histological subtypes of lung adenocarcinomas.

Table S2 Correlations between the expression levels of E-cadherin and ZEB1 and clinicopathological factors in non-small cell carcinoma ($n = 157$).

Table S3 Multivariate analysis of the clinicopathological factors correlated with the positive expression of ZEB1.



RESEARCH

Open Access

Histological comparison between preoperative and surgical specimens of non-small cell lung cancer for distinguishing between “squamous” and “non-squamous” cell carcinoma

Tomoko Yamagishi^{1†}, Katsuhiko Shimizu^{2†}, Nobuaki Ochi^{1†}, Hiromichi Yamane^{1†}, Isao Irei^{3†}, Yoshito Sadahira^{3†}, Nagio Takigawa^{1†}, Mikio Oka^{4†} and Masao Nakata^{2†}

Abstract

Background: Non-small cell lung cancers (NSCLCs) are frequently heterogeneous and in approximately 70% of cases, NSCLCs are diagnosed and staged by small biopsies or cytology rather than by examination of surgically resected specimens. Thus, in most patients, the diagnosis is established based on examination of preoperative specimens alone. Recently, classification of NSCLC into pathologic subtypes has been shown to be important for selecting the appropriate systemic therapy, from both the point of view of treatment efficacy and prevention of toxicity.

Methods: We retrospectively reviewed the data of 225 patients to compare the preoperative classification of the NSCLC subtype on biopsy specimens with the postoperative classification based on examination of the resected specimens, in order to compare the accuracy of the two for the diagnosis of various histological subtypes of NSCLC.

Results: In 169 of the 225 (75.1%) patients, the preoperative diagnosis was definite malignancy. Histologically, the final pathologic diagnosis made from the surgical specimens was adenocarcinoma (ADC) in 169 patients, and in 75.5% of these cases, the diagnosis was concordant with the preoperative diagnosis. Among the patients who had squamous cell carcinoma (SQC) in the preoperative specimens, the diagnosis was concordant with the preoperative diagnosis in 65.7% of cases. Misclassified preoperative biopsies included an even number of SQCs and ADCs, with all the misclassified biopsies being ADCs morphologically mimicking SQC due to solid growth. Significantly higher specificity, negative predictive value and accuracy were observed for the diagnosis of SQC.

Conclusions: Our study suggested that the concordance rates for diagnosis of the NSCLC subtypes, especially the “squamous” or “non-squamous” histologies, between preoperative and surgical specimens were satisfactory, as compared with previous reports. Therefore, pretreatment diagnosis of lung cancer using small samples is reasonable for selecting the optimal treatment. However, in order not to lose the opportunity for selecting an effective treatment, we should be aware that the diagnosis in preoperative small samples might be different from that based on examination of the surgical specimens.

Virtual Slides: The virtual slide(s) for this article can be found here: <http://www.diagnosticpathology.diagnomx.eu/vs/2032698427120488>

* Correspondence: kshimizu@med.kawasaki-m.ac.jp

[†]Equal contributors

²Department of General Thoracic Surgery, Kawasaki Medical School, 577 Matsushima, Kurashiki, Okayama 701-0192, Japan

Full list of author information is available at the end of the article



© 2014 Yamagishi et al.; licensee BioMed Central Ltd. This is an Open Access article distributed under the terms of the Creative Commons Attribution License (<http://creativecommons.org/licenses/by/4.0>), which permits unrestricted use, distribution, and reproduction in any medium, provided the original work is properly credited. The Creative Commons Public Domain Dedication waiver (<http://creativecommons.org/publicdomain/zero/1.0/>) applies to the data made available in this article, unless otherwise stated.

Background

Lung cancer is the leading cause of cancer and mortality from cancer worldwide [1], with 5-year survival rates of <15% across all stages of the disease [2]. Historically, lung cancer is divided into two morphologic types: small cell lung cancer and non-small-cell lung cancer (NSCLC), with NSCLC accounting for approximately 80% to 85% of all histological types of NSCLC [3].

The International Association for the Study of Lung Cancer, the American Thoracic Society, and the European Respiratory Society recently proposed the classification of NSCLC based on examination of small biopsy and/or cytology specimens into six main subtypes: adenocarcinoma (ADC), squamous cell carcinoma (SQC), NSCLC not otherwise specified (NSCLC-NOS), NSCLC with neuroendocrine morphology, NSCLC with squamous and adenocarcinoma patterns, and poorly differentiated NSCLC with spindle and/or giant cell carcinoma [4]. NSCLCs are frequently heterogeneous and approximately 70% of NSCLCs are diagnosed and staged by examination of small biopsy or cytology specimens rather than by examination of surgically resected specimens [5]; thus, in most patients, the diagnosis is based on examination of preoperative specimens alone. Until now, histological subtyping of NSCLC was not considered to be clinically or therapeutically important, because of the lack of existence of differential treatment options for the various subtypes of NSCLC. However, there is now clear

evidence to suggest that the classification of NSCLC into pathologic subtypes is important for the selection of appropriate systemic therapy, from both the point of view of treatment efficacy and prevention of toxicity [6,7]. For example, large phase III clinical trials have demonstrated that ADC is a strong predictive factor for improved outcome following treatment with the combination of pemetrexed with cisplatin compared with SQC [8]. In addition, the presence of common activating mutations in the tyrosine kinase domain of the epidermal growth factor receptor (*EGFR*) gene (exon 19 deletion and exon 21 L858R mutation) confers strong sensitivity to gefitinib and erlotinib, which are selective tyrosine kinase inhibitors of *EGFR* [9,10]. These *EGFR* mutations are more commonly encountered in ADCs [11]. Furthermore, the use of vascular endothelial growth factor (VEGF) inhibitors (eg, bevacizumab) has been demonstrated to be associated with an increased risk of fatal pulmonary hemorrhage in patients with SQC [12]. The *ALK* tyrosine inhibitor crizotinib was demonstrated to show marked antitumor activity in NSCLC patients with *EML4-ALK* translocation, observed in approximately 3 to 4% of patients with ADC [13]. Thus, a molecular testing guideline has been proposed [14].

If pathological findings are missed, especially when differentiating between “squamous” and “non-squamous” histology, determination of the appropriate treatment is difficult. The aim of this study was to compare the

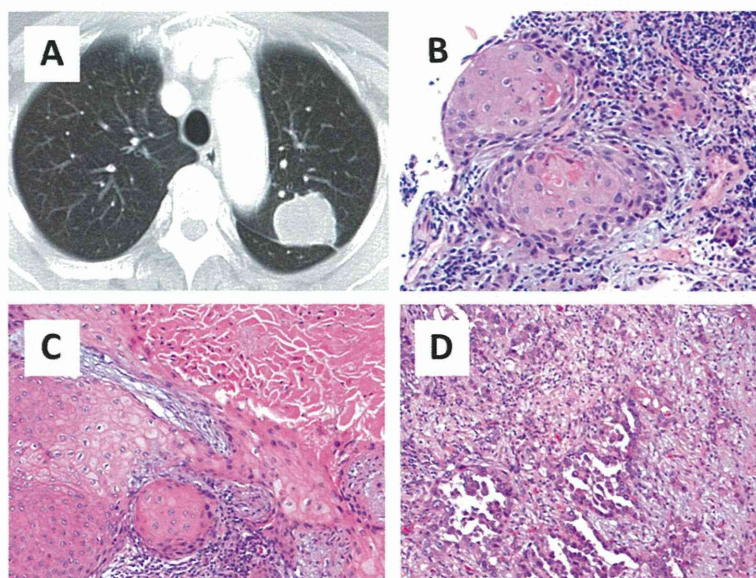


Figure 1 A case with discordant diagnosis of the histological subtype between preoperative and surgical specimens. (A) Computed tomographic image showing a mass lesion measuring 4 cm in diameter in the left upper lobe. (B) Computed tomography-guided fine needle biopsy was performed. Pathological findings of the biopsy specimen showed keratinized cells, suggestive of squamous cell carcinoma (H.E. stain, $\times 100$). (C-D) Surgically resected specimen showing both a squamous and glandular component, suggesting the postoperative diagnosis of adenosquamous carcinoma (H.E. stain, $\times 100$).

preoperative classification of NSCLC based on biopsy specimens with the postoperative classification made on the basis of examination of resected specimens, and to examine how often accuracy about each histological subtypes of NSCLC.

Methods

Patient population

Between April 2004 and June 2011, 442 patients underwent surgical resection for lung cancer at Kawasaki Medical School Hospital, Kurashiki, Japan. We retrospectively reviewed the data of a consecutive series of 225 (50.9%) patients in whom preoperative diagnosis was made by transbronchial biopsy (TBB) or computed tomography-guided fine needle biopsy (CTNB). For each patient, the clinical information at diagnosis was collected from the medical records. This study was conducted with the approval of the institutional Ethics Committee of Kawasaki Medical School (No.887).

Transbronchial biopsy and computed tomography-guided fine needle biopsy procedures

While TBB is commonly performed in the diagnostic workup of pulmonary peripheral nodules, CTNB is usually performed either when the tumor is not detected bronchoscopically or when it is thought unlikely to be accessible by bronchoscopy. Flexible bronchoscopy is conducted by experienced bronchoscopists, while CTNB is performed by interventional radiologists, with standard techniques for both. All aspirated materials and biopsy specimens were fixed in formalin and embedded in paraffin, and sections are routinely stained with hematoxylin and eosin (H&E). Cytological examinations of sputum, aspirated material and bronchial brushings, and washing were not included in the diagnostic workup in this study, because the aim of the study was histological comparison between preoperative biopsy specimens and surgically resected specimens.

The results of the examination of the small diagnostic specimens were classified as no malignancy, suspected malignancy or definite malignancy. Furthermore, definite malignancy of NSCLC was classified into ADC, SQC, NSCLC or other histological subtypes (others). If there is no clear ADC or SQC morphology, the tumor can be further classified based on immunohistochemical stains (IHC) and mucin (periodic acid Schiff) stains. If the stains all favor ADC: positive ADC markers (i.e., TTF-1 and/or mucin positive) with negative SQC markers, then the tumor is classified as ADC. If SQC markers (i.e., p63) are positive with negative ADC markers, the tumor is classified as SQC. If the ADC and SQC markers are both strongly positive and negative, the tumor is classified as NSCLC-NOS and others.

Table 1 Patient characteristics (n = 225)

Variable	Number	%
Age, mean ± SD	69.0 ± 10.2	
Sex		
Male	159	70.7
Female	66	29.3
Histology		
Adenocarcinoma	139	61.5
Squamous cell	67	30.1
NSCLC-NOS	10	4.4
Pleomorphic	5	2.2
Adenosquamous	4	1.8
Pathological stage		
IA	78	34.5
IB	53	23.9
IIA	23	10.2
IIB	24	10.6
IIIA	36	15.9
IIIB/IV	11	4.9

Abbreviations: NSCLC-NOS Non-small-cell lung carcinoma not otherwise specified.

Statistical analysis

Sensitivity, specificity, positive predictive value (PPV), negative predictive value (NPV), and accuracy were calculated according to the standard definitions for the diagnosis of lung cancer and malignancy. Continuous variables were analyzed by the Student's *t*-test, and the results were expressed as mean ± standard deviation (SD). Dichotomous variables were analyzed by the Fisher's exact test or the χ^2 test, as appropriate. Discontinuous variables were coded as dummy variables. Two-sided *p*-values of less than 0.05 were considered to be statistically significant. All analyses were performed using the SPSS software (Version 17.0; SPSS Incorporation, Chicago, IL).

Table 2 Comparison between preoperative specimens and surgical diagnosis

Preoperative diagnosis	Postoperative diagnosis					Total
	ADC	SQC	NSCLC-NOS	ASC	PLE	
Malignant						
ADC	105	3	2	3	2	115
SQC		44		1		45
NSCLC-NOS	2	1	4			7
PLE					2	2
Suspicious of NSCLC	5	7	1			13
Not malignant	27	12	3		1	43
Total	139	67	10	4	5	225

Abbreviations: ADC adenocarcinoma, SQC squamous cell carcinoma NSCLC-NOS non-small-cell lung cancer not otherwise specified, ASC adenosquamous carcinoma, PLE pleomorphic carcinoma.

Table 3 Diagnostic value of preoperative diagnosis between adenocarcinoma and squamous cell carcinoma

	Sensitivity (%)	Specificity (%)	PPV (%)	NPV (%)	Accuracy (%)
Lung cancer	75.1 (169/225)	-	100 (169/169)	100 (56/56)	75.1 (169/225)
ADC	75.5 (105/139)	88.3 (76/86)	91.0 (105/115)	69.0 (76/110)	80.4 (181/225)
SQC	65.6 (44/67)	99.3 (157/158)	97.7 (44/45)	87.2 (157/180)	89.3 (201/225)
p-value (ADC vs. SQC)	0.138	<0.001	0.184	<0.001	0.012

Abbreviations: PPV Positive predictive value, NPV Negative predictive value, ADC adenocarcinoma, SQC squamous cell carcinoma.

Results

Case report

A 74-year-old woman who was a never-smoker was referred to our hospital because of hoarseness. Computed tomography showed a solid mass approximately 4 cm in diameter in the left upper lobe associated with mediastinal lymphadenopathy (Figure 1A). CTNB was carried out, and biopsy examination confirmed a well-keratinized tumor without obvious glandular features or cytoplasmic mucin (Figure 1B). The patient was diagnosed as having SQC of the lung, stage IIIA (T2aN2M0). Left upper lobectomy with mediastinal lymph node dissection was performed. Both ADC and SQC components were observed in the pathological specimen, suggesting the postoperative diagnosis of adenosquamous carcinoma (Figure 1C&D). One year later, recurrence was found in the form of mediastinal lymphadenopathy. We performed a molecular analysis of the surgical specimens, which revealed an *EGFR* gene mutation, and treatment with oral gefitinib was initiated. The patient would have lost the opportunity to receive gefitinib treatment if had just been diagnosed as having inoperable advanced NSCLC, because the molecular testing guideline does not recommend *EGFR* mutation analysis in patients with SQC [14].

Patient characteristics

A total of 225 patients (159 men and 66 female; mean age, 69.0 ± 10.2 years) were enrolled in this study. The pathological stage and histological type on the final

pathological examination are shown in Table 1. The most frequent histological type was ADC; 139 (61.5%) had ADC, 67 (30.1%) had SQC, 10 (4.4%) had large cell carcinoma, and 9 (4.0%) had others (other subtypes). The patients were classified according to the histopathological stage as follows: 131 patients had stage I, 47 had stage II, and 47 had stage III or IV disease. Most stage III and IV patients were recognized during and after surgery due to mediastinal lymph node metastasis (cN0-pN2) and pleural dissemination (cM0-pM1a). A few stage III patients were performed resection due to single mediastinal lymph node metastasis.

Sensitivity of preoperative diagnosis for the detection of NSCLC

The preoperative diagnosis was compared with the final pathological findings (Table 2). In 169 of the 225 (75.1%) patients, the preoperative diagnoses were definite malignancy (115 ADC, 45 SQC, 2 large cell carcinoma, 2 pleomorphic carcinoma, and 5 NSCLC). In 56 of the 225 (24.9%) patients, the preoperative specimens showed suspected or no malignancy: while NSCLC was suspected preoperatively in 13 of these patients, no malignancy was suspected in 43 patients. The overall sensitivity for the detection of lung cancer was 75.1%.

Histologically, the final pathological examination of the surgical specimens revealed ADC in 139 patients, of whom in 105 (75.5%) patients, the diagnosis was concordant with the preoperative diagnosis. Of the remaining 34

Table 4 Comparison of H&E stain vs IHC for subtyping NSCLC

Postoperative diagnosis	Preoperative diagnosis							
	H&E diagnosis				IHC predicted phenotype			
	ADC	SQC	Unclassified	Total	ADC	SQC	Unclassified	Total
ADC	79		28	107	26			26
SQC	2	40	6	48	1	3		4
Unclassified	5	2	7	14	2		3	5
Total	86	42	41	169	29	3	3	35

Abbreviations: ADC adenocarcinoma, SQC squamous cell carcinoma, NSCLC-NOS non-small-cell lung cancer not otherwise specified, PLE pleomorphic carcinoma, H&E hematoxylin and eosin, IHC immunohistochemistry.

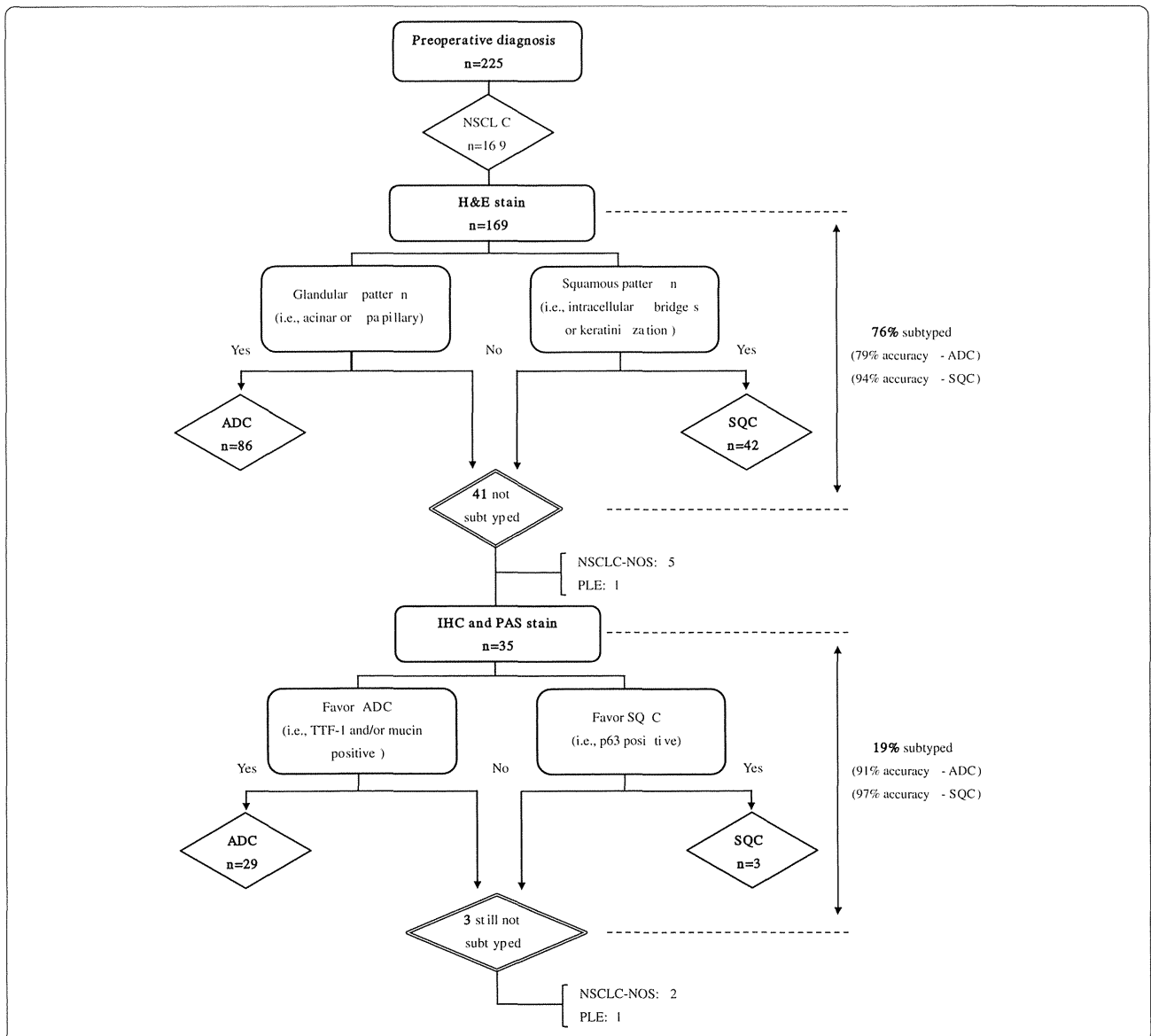


Figure 2 Diagnostic algorithm for classification of NSCLC in preoperative specimens.

patients, 2 patients had NSCLC, 5 patients had suspected NSCLC, and 27 patients had no malignancy. In all, 67 patients had SQC of the lung on the preoperative specimens, and in 44 (65.7%) of these patients, the diagnosis was concordant with the preoperative diagnosis. Among the 23 of the remaining 67 (34.3%) with a discordant diagnosis, 3 patients had ADC, 1 patient had NSCLC, 7 patients had suspected NSCLC and 12 patients had no evidence of malignancy. Misclassified preoperative biopsies included an even number of SQCs and ADCs (n = 3), whereas all of the misclassified biopsies were ADC, morphologically mimicking SQC due to the solid growth.

We compared the sensitivity, specificity, predictive values and accuracy for the diagnosis of ADC and SQC

(Table 3). Significantly higher specificity, NPV and accuracy were observed for SQC (p < 0.05).

Comparison of H&E stain vs. IHC for subtyping NSCLC

For the comparison of H&E stain vs IHC, 169 patients were included, all of whom underwent H&E stain. Among them, IHC was performed on 35 (21%) patients (Table 4). As summarized in Figure 2, 128 of 169 patients (76%) were specifically subtyped on the H&E stain as either ADC or SQC. 41 (24%) patients were not subtyped on the H&E stain sections. IHC could successfully subtype NSCLC in 32 of 35 cases (29 ADC, 3 SQC). The remaining three cases were not still subtyped (2 NSCLC-NOS, 1 PLE). However, by combining the results of the two methods,

Table 5 Comparison of TBB vs. CTNB for sensitivity/concordance rate

	Histological diagnosis			Sensitivity	p-value	Concordance	p-value
	Lung cancer	Suspicious of malignancy	No malignancy				
TBB	140	13	37	73.2 (140/190)	0.249	66.8 (127/190)	0.594
CTNB	29	0	6	82.9 (29/35)		71.4 (25/35)	
Total	169	13	43	75.0 (169/225)		67.6 (152/225)	

Abbreviations: TBB Transbronchial biopsy, CTNB Computed tomography-guided fine needle biopsy.

the number of patients with not subtyped diagnoses was reduced to 9 (5%) patients. The accuracy of both morphologic differentiation and IHC based predictive subtype is <100% (Figure 2).

Comparison of TBB vs. CTNB for the sensitivity or concordance of lung cancer diagnosis

Among the 225 patient studied, TBB was performed in 190 patients. Of these, 140 (73.7%) were diagnosed as having definite lung cancer, 13 (6.8%) were suspected as having malignancy, and 37 (19.5%) were diagnosed as having no malignancy. CTNB was performed in 35 patients. Of these, 29 (82.9%) and 6 (17.1%) cases were diagnosed as having lung cancer and no malignancy, respectively. Thus, there was no significant difference in the level of diagnostic certainty between TBB and CTNB (Table 5).

Comparison of the sensitivity or concordance rate of the histological type between preoperative and surgical specimens in relation to the tumor size

The results of detection of lung cancer were correlated with the tumor size. The overall sensitivity and concordance rate of histological type between preoperative biopsies and surgical specimens were 75.1% (169/225) and 67.6% (152/225). The sensitivity rate was correlated with the tumor size. The diagnostic sensitivity of lesions larger than 2.1 cm in diameter was significantly better than that of lesions less than 2 cm in diameter (p = 0.001, Table 6). However, concordance rate was not correlated with the tumor sizes.

Discussion

We assessed the accuracy of diagnosis of the histological type of lung cancer between preoperative and surgical specimens. The reported accuracy for bronchoscopic biopsy as compared to histopathology of resected or autopsy specimens for differentiating among histological

subtypes of lung cancer is in the range of 62% to 97.5% [15-19]. In our study, the concordance rates for diagnosis of the NSCLC subtypes between preoperative biopsies and histopathology of surgical specimens was 66.8% (127/190), which seemed to be slightly low as compared to previous reports; however, many studies excluded tumors that were confirmed as not being malignant: in our study, 50 (26.3%) of 190 patients were diagnosed as not having malignant lesions before excision. After patients without malignancies as determined in preoperative specimens were excluded, the concordance rate was 90.7% (127/140). We found a better accuracy for the diagnosis of SQC than for that of ADC (89.3% vs. 80.4%, p = 0.012), which was also in agreement with previous studies [13,20]. On the other hand, the sensitivity for ADC was slightly better than that for SQC (75.7% vs. 65.6%, p = 0.138), indicating that ADC seems to have little oversight by preoperative specimens.

IHC studies are usually required if obvious morphological features of squamous or glandular differentiation are not identified. Similar to the findings of this study, prior studies found that ~75% of bronchial NSCLC samples may be subtyped using morphology alone, and 93% of all NSCLC cases may be subtyped when combined immunostaining [21]. Other studies also demonstrated that only a low population (6%) of cases remained without a probable subtype after morphologic examination and IHC [22]. The low not-typed rate in these studies suggests that we should perform IHC as a routine utilization for subtyping of difficult cases.

Several factors affect the diagnostic accuracy. The frequency of diagnostic errors induced by some of these factors, including the biopsy size and degree of differentiation has been described [20]. In our study, the tumor size was correlated with the sensitivity and concordance rate: the larger the diameter, the greater the sensitivity and cell type agreement.

Table 6 Comparison between tumor size and sensitivity/concordance rate

	Histological diagnosis			Sensitivity	p-value	Concordance	p-value
	Lung cancer	Suspicious of malignancy	No malignancy				
<=2 cm	30	0	19	61.2 (30/49)	0.011	57.1 (28/49)	0.078
>2 cm	139	13	24	78.9 (139/176)		70.4 (124/176)	
Total	169	13	43	75.0 (169/225)		67.6 (152/225)	

Until date, therapeutic decisions are heavily dependent on the histological subtype of lung cancer (SQC vs. non-SQC) and its molecular characteristics (e.g., *EGFR* mutation and *ALK* rearrangement states). Furthermore, many previous studies showed the expression and functions of proteins and genes in lung cancer, and it may be significantly related to tumor progression and metastasis [23-26].

Both *EGFR* mutation and *ALK* rearrangements are almost exclusively seen in ADC. According to multiple large phase III clinical trials [11,27-29], the new classification recommends that all patients with advanced lung ADC be tested for *EGFR* mutation, as *EGFR* tyrosine kinase inhibitors can be used as first-line chemotherapy for patients with *EGFR* mutations. Crizotinib has been approved by the US Food and Drug Administration (FDA) for advanced ADC with *ALK* rearrangements [30]. Therefore, testing for *EGFR* mutations and *ALK* rearrangements in patients with advanced ADC is no longer only a research tool, and should be performed in clinical practice. On the other hand, several molecular targets such as *FGFR1* amplification and *DDR2* mutation have been discovered in SQC [31,32]. Target therapies that might be beneficial in this selected subpopulation have never been reported. These results indicate that misdiagnosis of ADC as SQC in preoperative specimens should be avoided so as to prevent the loss of opportunity to select beneficial molecular-targeted therapy for these patients in clinical practice. Although such a result was not seen, there were three (1.3%) misclassifications between ADC and SQC in the preoperative specimens, and in all, SQC was diagnosed as ADC. Fortunately, there was only a lone patient who might have lost the opportunity to receive *EGFR*-TKI therapy by missed diagnosis (0.44%, shown as case report).

Our retrospective study had some limitations. First, only half of the patients who underwent surgery received preoperative diagnosis by TBB or CTNB. Second, there may be variability between intra- and inter- pathologist in lung cancer diagnosis. Because a smaller amount of tissue is obtained, the diagnostic assessment might be more difficult and more inconsistent in the diagnosis of pathologists might occur. In such cases, multidisciplinary approach and expert consultation are recommended [33].

Conclusions

In conclusion, our study suggested that the concordance rate for the diagnosis of NSCLC subtypes, especially “squamous” or “non-squamous” histology, between preoperative and surgical specimens was satisfactory as compared with other reports. Pretreatment diagnosis of lung cancer using small samples is reasonable for selection of the optimal treatment. However, our case report presented above serves to emphasize the need to be

aware that diagnosis based on preoperative small samples might be different from that made from surgical specimens, so as to not lose the opportunity for effective treatment.

Consent

Written informed consent was obtained from the patient for the publication of this report and any accompanying images.

Competing interests

The authors declare that they have no competing interests.

Authors' contributions

TY and KS designed and wrote the paper. NO, HY, NT and MO participated in the design of the study and reviewed the literature. KS and MN performed surgery. All authors read and approved the final manuscript.

Author details

¹Department of General Internal Medicine 4, Kawasaki Medical School, 2-1-80, Nakasange, Kita-ku, Okayama 700-8505, Japan. ²Department of General Thoracic Surgery, Kawasaki Medical School, 577 Matsushima, Kurashiki, Okayama 701-0192, Japan. ³Department of Pathology, Kawasaki Medical School, 577 Matsushima, Kurashiki, Okayama 701-0192, Japan. ⁴Department of Respiratory Medicine, Kawasaki Medical School, 577 Matsushima, Kurashiki, Okayama 701-0192, Japan.

Received: 5 February 2014 Accepted: 15 May 2014

Published: 29 May 2014

References

1. Jemal A, Bray F, Center MM, Ferlay J, Ward E, Forman D: Global cancer statistics. *CA Cancer J Clin* 2011, **61**:69-90.
2. Crino L, Weder W, Van Meerbeek J, Felip E: Early stage and locally advanced (non-metastatic) non-small-cell lung cancer. ESMO clinical practice guidelines for diagnosis, treatment and follow-up. *Ann Oncol* 2010, **21**:1103-1.
3. Itaya T, Yamaoto N, Ando M, Ebisawa M, Nakamura Y, Murakami H, Asai G, Endo M, Takahashi T: Influence of histological type, smoking history and chemotherapy on survival after first-line therapy in patients with advanced non-small cell lung cancer. *Cancer Sci* 2007, **98**:226-230.
4. Travis WD, Brambilla E, Noguchi M, Nicholson AG, Geisinger KR, Yatabe Y, Beer DG, Powell CA, Riely GJ, Van Schil PE, Garg K, Austin JH, Asamura H, Rusch WW, Hirsch FR, Scagliotti G, Mitsudomi T, Huber RM, Ishikawa Y, Jett J, Sanchez-Cespedes M, Sculier JP, Takahashi T, Tsuboi M, Vansteenkiste J, Wistuba I, Yang PC, Aberle D, Brambilla C, Flieder D, et al: International association for the study of lung Cancer/American thoracic Society/European respiratory society international multidisciplinary classification of lung adenocarcinoma. *J Thorac Oncol* 2011, **6**:244-285.
5. Shah PL, Singh S, Bower M, Livni N, Padley S, Nicholson AG: The role of transbronchial fine needle aspiration in an integrated care pathway for the assessment of patients with suspected lung cancer. *J Thorac Oncol* 2006, **1**:324-327.
6. Einhorn LH: First-line chemotherapy for non-small-cell lung cancer: is there a superior regimen based on histology? *J Clin Oncol* 2008, **20**:3485-3486.
7. Stinchcombe TE, Grilley-Olson JE, Socinski MA: If histology matters. *J Clin Oncol* 2010, **28**:1810-1812.
8. Scagliotti GV, Parikh P, Von Pawel J, Biesma B, Vansteenkiste J, Manegold C, Serwatowski P, Gatzemeier U, Digumarti R, Zukin M, Lee JS, Mellemaard A, Park K, Patil S, Rolski J, Goksel T, De Marinis F, Simms L, Sugarman KP, Gandara D: Phase III study comparing cisplatin plus gemcitabine with cisplatin plus pemetrexed in chemotherapy-naïve patients with advanced-stage non-small-cell lung cancer. *J Clin Oncol* 2008, **26**:3543-3551.
9. Lynch TJ, Bell DW, Sordella R, Gurubhagavatula S, Okimoto RA, Brannigan BW, Harris PL, Haserlat SM, Supko JG, Haluska FG, Louis DN, Christiani DC, Settleman J, Haber DA: Activating mutations in the epidermal growth factor receptor underlying responsiveness of non-small-cell lung cancer to gefitinib. *N Engl J Med* 2004, **350**:2129-2139.